Electronic structure of $LaCrO_3$, $LaMnO_3$ and $LaFeO_3$ from ***ab initio*** spin-polarized calculations

1997 J. Phys.: Condens. Matter 9 3129

(http://iopscience.iop.org/0953-8984/9/15/006)

J. Phys.: Condens. Matter **9** (1997) 3129–3138. Printed in the UK PII: S0953-8984(97)79191-4

Electronic structure of $LaCrO_3$, $LaMnO_3$ and $LaFeO_3$ from *ab initio* spin-polarized calculations

Priya Mahadevan†‡, N Shanthi† and D D Sarma†§

† Solid State and Structural Chemistry Unit, Indian Institute of Science, Bangalore 560012, India
‡ Department of Physics, Indian Institute of Science, Bangalore 560012, India

Received 4 November 1996

Abstract. The electronic structures of the $LaMO_3$ series are discussed on the basis of *ab initio* band-structure calculations within the local spin-density approximation, which correctly predicts the insulating and magnetic structures in each case. The band dispersions obtained along various symmetry directions were mapped onto those calculated with a nearest-neighbour tight-binding model within a least-squared-error procedure, providing estimates for the various hopping strengths as well as the intra-atomic exchange strength in each case.

1. Introduction

The electronic structures of strongly correlated transition metal oxides have been traditionally described within various model many-body Hamiltonians incorporating the effects of different hopping interactions, charge-transfer processes and Coulomb interaction strengths [1–3]. Applications of such parametrized model many-body approaches, however, require a prior knowledge of the various interaction strengths; for example, in the context of a multiband Hubbard model, one requires the intra-atomic Coulomb strength U_{dd}, the charge-transfer energy Δ, and the metal d–oxygen p hopping interaction strength t. These quantities are often estimated from analysis of high-energy spectroscopic results in conjunction with such model Hamiltonian calculations. This method of estimation of parameters, however, leads to non-unique solutions, as a wide range of parameters can reproduce the same experimental spectrum [4]. Even if only one interaction strength can be reliably estimated from any other method, the problem of non-uniqueness in analysing experimental spectroscopic results is considerably eliminated, and such an approach will yield a more consistent description of the electronic structure.

It has been recently shown [5, 6] that *ab initio* band-structure calculations provide a reasonable starting point for the description of the electronic structure of $LaMO_3$ (M = Cr–Ni). Not only do these calculations predict the correct magnetic structure for these systems, but the excitation spectra are also well described [5]. This has further prompted the extraction of various electronic interaction strengths by analysing the *ab initio* band dispersions in terms of a tight-binding (TB) model for the $LaMO_3$ series with M = Ti–Ni [7]. However, in this work only spin-restricted calculations based on the local density approximation were performed for the analysis. This is suitable for the two compounds in the $LaMO_3$ series, namely $LaCoO_3$ and $LaNiO_3$, since these two compounds have non-magnetic ground states. In contrast, other $LaMO_3$ compounds with M = Cr–Fe have

§ Also at: Jawaharlal Nehru Centre for Advanced Scientific Research, Bangalore 560012, India.

0953-8984/97/153129+10$19.50

various antiferromagnetic ground states. Thus it is desirable to analyse the spin-polarized calculations on the basis of local spin-density approximation (LSDA) in order to obtain reliable electronic interaction strengths relevant for the near-ground-state properties of these materials. Moreover, analysis of any spin-restricted calculations cannot yield any magnetic information and, specifically, cannot provide an estimate of the intra-atomic exchange interaction strength J, which plays a crucial role in stabilizing a magnetic moment and thus a magnetic structure in these oxides. It has indeed been recently shown [5] that the presence of a large J is crucial for the unusual electronic structure and very interesting physical properties (such as colossal magnetoresistance) in compounds based on $LaMnO_3$. In view of these considerations, we have analysed the band dispersions obtained from *ab initio* spin-polarized LSDA calculations for the three compounds $LaCrO_3$, $LaMnO_3$ and $LaFeO_3$ in terms of a tight-binding model. In this way we have obtained estimates of various interaction strengths including J for these compounds.

2. Methodology

Band-structure calculations within the LSDA were performed for the oxides $LaMO_3$ (M = Cr–Fe) using the linearized muffin-tin orbital (LMTO) [8] method within the atomic sphere approximation (ASA). We have used the real crystal structures with 20 atoms in the unit cell in each case with structural data obtained from the following references: $LaCrO_3$: [9]; $LaMnO_3$: [10]; and $LaFeO_3$: [11]. Earlier works have already shown [6] that LSDA calculations predict the magnetic structure correctly for each of these three compounds. In each case, we consider only those calculations which correspond to the observed magnetic ground state, as we are interested in extracting various electronic interaction strengths relevant for the near-ground-state properties of these compounds. Thus, the calculations were for the G-type antiferromagnetic structure for $LaCrO_3$ and $LaFeO_3$, and for the A-type antiferromagnetic arrangement in the case of $LaMnO_3$. The scalar relativistic spin-polarized band-structure calculations were carried out for 216 points in the Brillouin zone. We have included the s, p, d and f basis in each atomic sphere. However, the basic electronic structures of these transition metal oxides are essentially controlled by the transition metal d and oxygen p interactions. Thus, while mapping the results onto a nearest-neighbour tight-binding model, we have restricted the basis set to the transition metal d and the oxygen p orbitals only. However, in order to simulate the crystal-field splitting at the Γ point, it was found necessary to include the s orbitals on the oxygen [13]. All hopping interactions were parametrized within the Slater–Koster scheme [12]. Thus, oxygen p–oxygen p interactions are characterized by two parameters, ppσ and ppπ, and oxygen p–transition metal d interactions are expressed in terms of pdσ and pdπ. The parameter sdσ simulates the extent of t_{2g}–e_g splitting at the Γ point via the s–d interaction.

In order to obtain the magnetic ground state within the single-particle tight-binding model, we have introduced an extra parameter, ϵ_{pol}, which is the bare energy difference between the up- and down-spin d electrons at the same site. It is also necessary to include the effect of non-orthogonality of atomic functions located at different sites by considering the overlap matrix in such tight-binding approaches [7, 13]. However, the tight-binding part of any parametrized many-body Hamiltonian ignores the overlap matrix with an assumption of orthogonality of basis functions. Since we are eventually interested in obtaining the estimates of the interaction strengths that enter such many-body Hamiltonians as parameters, we have carried out the fitting of the LMTO dispersions within two separate tight-binding models, one with and the other without the assumption of orthogonal basis functions. The results of these two fitting procedures are consistent with each other.

As only transition metal d and oxygen p states are considered, there are 56 bands with primarily d and p characters to be fitted. Of these bands, the low-lying bands near the bottom of the nominal oxygen p bandwidths have non-negligible contribution from La-derived states. Therefore, we have not taken into account all of these bands in the fitting procedure. In the case of $LaCrO_3$, we leave out the top four bands as these overlap extensively with states arising from La orbitals. In the case of $LaFeO_3$ we have considered only the top 20 bands out of the 56 bands, since extensive overlap of primarily Fe d-derived states with the oxygen p band makes it difficult to identify the non-bonding oxygen bands.

Only in the case of $LaMnO_3$, which is a Jahn–Teller-distorted compound, are there two Mn–O distances, as well as a variation of the O–O distance over a range of 2.61–2.84 Å. In order to incorporate the effects of such variations in distances, the hopping interaction strengths were assumed to scale with distance in the form $1/r^x$. x is predicted to be equal to 3 and 4 for p–p and p–d interactions respectively, [14], though other choices have also been suggested [15]. In the context of the analysis of the spin-restricted calculations [7], we found that the dependence of the hopping interaction can be significantly different from all previous suggestions. Thus, we have treated x_{p-p} and x_{p-d} as parameters suitably optimized to obtain the best fit to the LMTO results of $LaMnO_3$.

3. Results and discussion

As a typical case in these transition metal perovskite oxides, we show the calculated total density of states (TDOS) and various partial densities of states (PDOS) for $LaCrO_3$ in figure 1 and the corresponding band dispersions along the high-symmetry lines in figure 2(a). In figure 1(a), we show the TDOS along with the partial Cr d and O p DOS, while figures 1(b) and 1(c) exhibit the spin-polarized Cr d PDOS from one Cr site in the antiferromagnetic unit cell. The other Cr site in the unit cell has precisely the same Cr d PDOS with the up-spin PDOS at one site being exactly the same as the down-spin PDOS of the other site and vice versa. This is of course a consequence of the antiferromagnetic structure in this compound. The TDOS exhibits a large bandgap ($\sim$1.13 eV) consistent with the insulating ground state of this compound. In figure 1 we find a broad group of DOS approximately between -7 and -3 eV; this DOS is dominantly contributed by oxygen p PDOS with small admixture of Cr d contributions (see figure 1(a)). This observation identifies this group of states as arising primarily from the oxygen p band. It can also be seen that the lower energy (between -7 and -5 eV) in this DOS range has relatively more Cr d contributions, while the Cr d contribution is nearly absent between -5 and -3 eV. This suggests that the latter energy region arises from primarily oxygen p–oxygen p interactions and can be termed as a non-bonding region with respect to oxygen p–transition metal d interactions. On the other hand, the larger contributions from Cr d states below -5 eV indicate that these states are substantially influenced by oxygen p–transition metal d interactions and, thus, this energy region is termed the bonding region with respect to p–d interactions. The p–d interactions in these materials with approximately cubic symmetry can be discussed within the ligand field theory [16]. Thus, we expect the transition metal d states to split into two groups of states, namely t_{2g} and e_g; each of these are further split by the exchange interaction into up- and down-spin states. Then these four states, i.e. $t_{2g\uparrow}$, $t_{2g\downarrow}$, $e_{g\uparrow}$, $e_{g\downarrow}$, interact with the suitably space- and spin-symmetry-adapted oxygen states to form four pairs of bonding and antibonding states due to p–d interactions. All of the four p–d bonding states energetically overlap in the energy range between -7 and -5 eV; this fact is also responsible for absence of any perceptible spin polarization in this energy range. In contrast, strong spin polarization and a substantial effective crystal-field

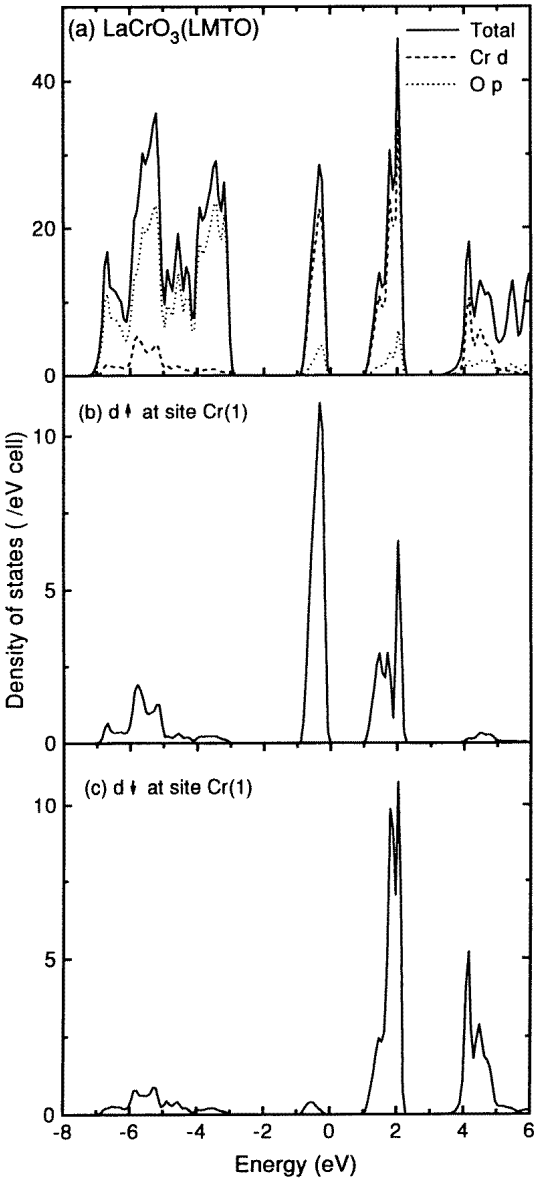

Figure 1. (a) The LMTO DOS for $LaCrO_3$ (solid line) as well as the PDOS for the oxygen p states (dotted line) and for the Cr d states (dashed line), along with (b) the up-spin and (c) the down-spin d PDOS from one Cr site in the antiferromagnetic unit cell.

splitting allow us to identify each of the four antibonding counterparts arising from the p–d interactions. Thus, the narrow DOS between −1 and 0 eV in figure 1 corresponds to the band dispersions in the same energy range shown in figure 2(a). There are six bands here in the unit cell and these are evidently due to Cr d $t_{2g\uparrow}$ states from site 1; the second Cr site has an identical distribution of the $t_{2g\downarrow}$ states, as discussed already. Clearly separated by an energy gap from these t_{2g} states is another group of up-spin states between 1 and 2.5 eV in

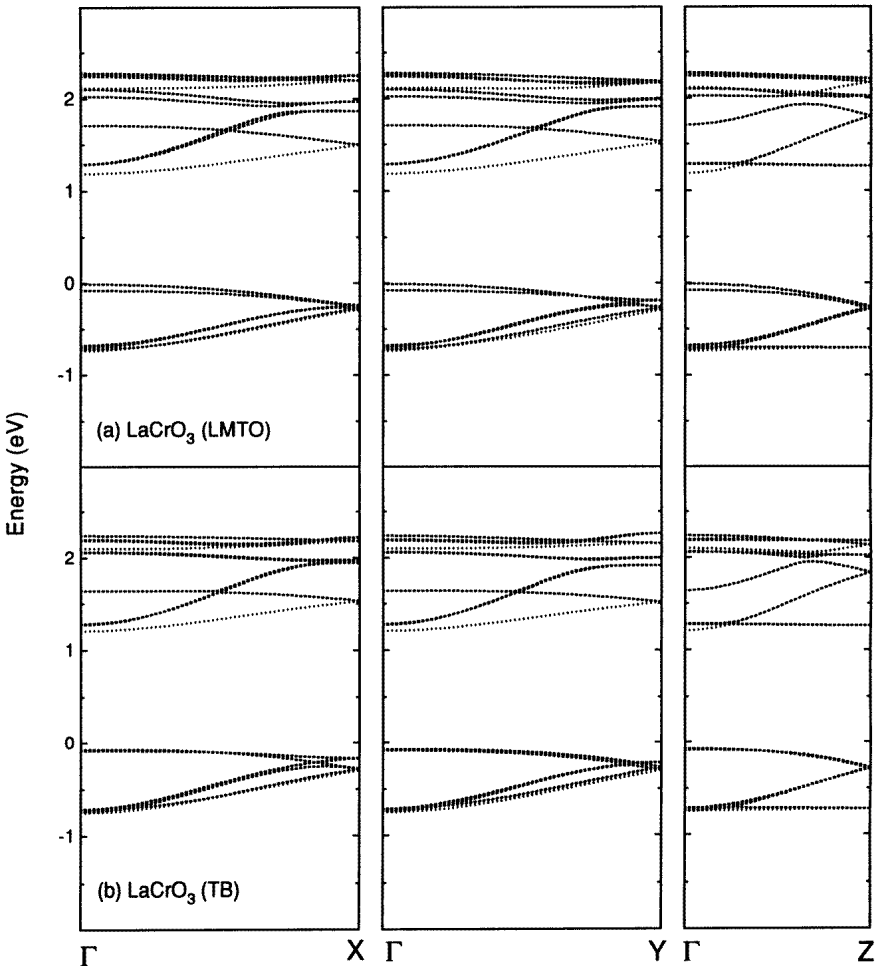

Figure 2. (a) The LMTO band dispersions, and (b) the best-fit TB band dispersions for $LaCrO_3$ along the symmetry directions ΓX, ΓY and ΓZ.

figure 1(b). Overlapping these states, we also find the first group of prominent down-spin states in figure 1(c). These latter states in figure 1(c) can be attributed to the $t_{2g\downarrow}$ states exchange-split from the $t_{2g\uparrow}$ states appearing between -1 and 0 eV in figure 1(b). The up-spin states in figure 1(b) between 1 and 2.5 eV are attributed to the $e_{g\uparrow}$ states split from the $t_{2g\uparrow}$ states by the crystal-field effects. Thus, in this compound the exchange splitting and the crystal-field splitting are approximately equal, leading to an energetic overlap between $t_{2g\downarrow}$ and $e_{g\uparrow}$ states of Cr d. Consequently, figure 2(a) shows ten bands dispersing within the energy interval of approximately 1 and 2.5 eV; out of these, approximately four bands show stronger dispersions compared to the remaining six. The TDOS (figure 1(a)) shows a broad group of states continuing above 4 eV; however, the Cr d contribution to this energy region is significant only between 4 and 5 eV. These Cr d states belong primarily to the down-spin states (figure 1(c)); thus, these are attributed to Cr d $e_{g\downarrow}$ states from Cr site 1. In the same energy range there is a significant contribution from states other than Cr d and O

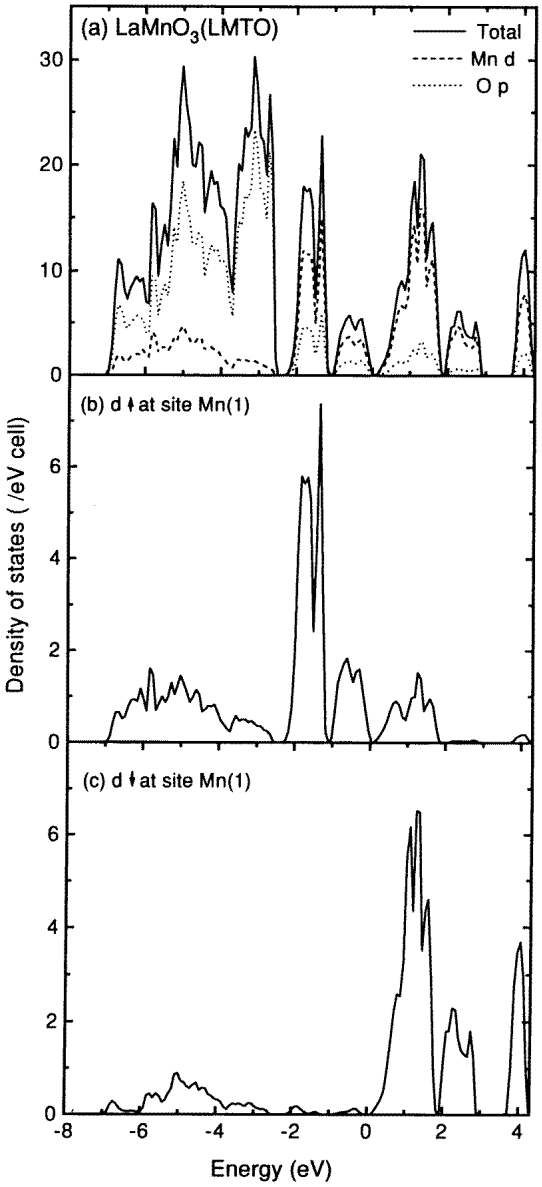

Figure 3. (a) The LMTO DOS for $LaMnO_3$ (solid line) as well as the PDOS for the oxygen p states (dotted line) and for the Mn d states (dashed line), along with (b) the up-spin and (c) the down-spin d PDOS from one Mn site in the antiferromagnetic unit cell.

p; PDOS calculations (not shown in the figure) suggest a dominant contribution from La d states. Thus the dispersions of the $e_{g\downarrow}$ states are overlapped by various dispersions arising from La d states and, consequently, it is not possible to identify the dispersions arising from the Cr d states in this energy range. This is why the dispersions (not shown in the figure) were left out of the TB fitting procedure as explained in the methodology section.

The other two compounds, $LaMnO_3$ and $LaFeO_3$, exhibit similar features in the

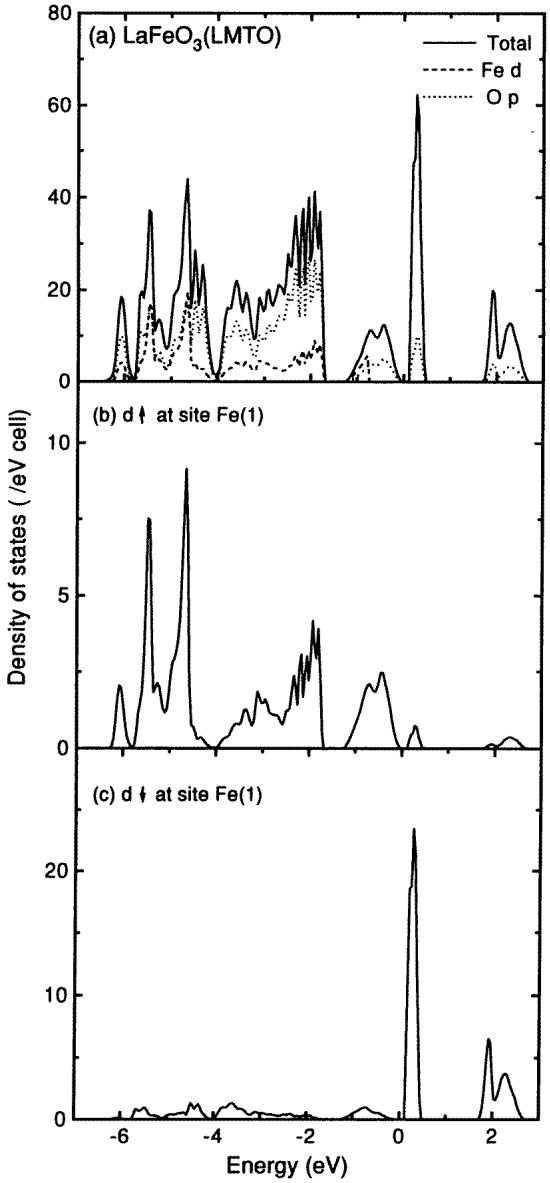

Figure 4. (a) The LMTO DOS for $LaFeO_3$ (solid line) as well as the PDOS for the oxygen p states (dotted line) and for the Fe d states (dashed line), along with (b) the up-spin and (c) the down-spin d PDOS from one Fe site in the antiferromagnetic unit cell.

respective TDOS and PDOS as shown in figures 3 and 4. Thus one can easily identify the oxygen bands between -7 and -2.5 eV in the case of $LaMnO_3$, in close similarity with that of $LaCrO_3$. However, there are some differences between the d-band-related features of the two compounds. The Cr d↑ as well as d↓ states are split into two groups of states with primarily t_{2g} and e_g symmetries due to the cubic crystal-field effects (figure 1). In contrast, the d-related features in $LaMnO_3$ are split into three groups as shown in figures

3(b) and 3(c). This arises from the Jahn–Teller distortion of the Mn–O_6 octahedra in this compound; this leads to a lowering of the local point-group symmetry O_h to D_{4h}, thereby splitting the t_{2g} of O_h symmetry into e_g and b_{2g} of D_{4h} symmetry and the e_g into b_{1g} and a_{1g} states. In the case of $LaFeO_3$, the dominant contribution in the energy range ~ -6 to -4 eV appears to be from the transition metal d states, while the region between -4 and -1.5 eV is dominated by the oxygen p states. Thus, it appears that at least a part of the transition metal d states in $LaFeO_3$ appears below the oxygen p states, unlike in the other two compounds; this gives rise to mixing between the Fe d↑ states at site 1 with the oxygen p states leading to an extensive redistribution of these states over a wide energy region as shown in figure 4(b). In contrast, Fe d↓ states, being pushed out of the oxygen p band due to the presence of strong exchange splitting, exhibit a simple t_{2g}–e_g splitting due to crystal-field effects (see figure 4(c)).

Table 1. Estimates of tight-binding parameters obtained by a least-squared-error fitting of LMTO results including orbital overlaps. The numbers in parentheses have been obtained by assuming an orthonormal basis. All energies are in electron volts (eV).

Compound	sdσ	ppσ	ppπ	pdσ	pdπ	$\epsilon_{d\uparrow} - \epsilon_{p\uparrow}$	ϵ_{pol}
$LaCrO_3$	−2.44	0.71	−0.15	−2.22	1.22	2.73	2.46
	(−2.37)	(0.55)	(−0.09)	(−2.10	(1.10)	(2.23)	(2.66)
$LaMnO_3$	−2.12	0.74	−0.20	−1.92	1.19	0.80	3.48
	(−2.36)	(0.58)	(−0.14)	(−2.08)	(1.16)	(0.65)	(3.71)
$LaFeO_3$	−1.47	0.69	−0.16	−1.56	0.90	−0.79	3.66
	(−1.4)	(0.74)	(−0.14)	(−1.64)	(0.74)	(−0.82)	(3.78)

We have fitted the LMTO band dispersions along the high-symmetry lines within the nearest-neighbour TB transition metal d–oxygen p model for each of the three compounds within a least-squared-error procedure as described in the methodology section. The resulting best-fit dispersions obtained from the TB method for $LaCrO_3$ are shown in figure 2(b) compared to the corresponding LMTO dispersions in figure 2(a). Similar fits to the band dispersions were obtained also for the other two compounds, $LaMnO_3$ and $LaFeO_3$. The parameter values that provide these best fits are given in table 1; the numbers in the parentheses are those obtained from the fitting procedure without considering any orbital overlap, i.e. under the assumption of orthogonality of the basis functions. We find some systematic trend in the parameter strengths. Thus, $\epsilon_d - \epsilon_p$ monotonically decreases across the series, being largest for $LaCrO_3$ and smallest for $LaFeO_3$. This is a consequence of the increasing atomic number and the consequent stabilization of the transition metal d level with increasing nuclear attraction. The strength of the p–d interaction is also found to decrease monotonically across the series. This is also a consequence of the increasing atomic number leading to a contraction of the d orbitals across the series. This is reflected in a decrease of both (pdσ) and (pdπ) interaction strengths. The ppσ and ppπ interaction strengths, which are related only to oxygen–oxygen interactions, do not change very much across the series; this is a result of the fact that the oxygen–oxygen distances are very similar in these three compounds: 2.73 Å in $LaCrO_3$, 2.66 Å in $LaMnO_3$ and 2.77 Å in $LaFeO_3$. It is interesting to note that the small variations in (ppσ) in these compounds reflect the small changes in the O–O distances in these compounds. The (sdσ) interaction on the other hand decreases systematically, reflecting a decreasing crystal-field splitting at the Γ point across the series.

Jahn–Teller distortion of the $LaMnO_3$ crystal structure leads to different metal–oxygen (M–O) and oxygen–oxygen (O–O) distances (r) within the first coordination shell of this

compound. In order to include the effect of changing distances on the hopping strengths, we need three extra parameters, x_{sd}, x_{pp} and x_{pd}, only in the case of $LaMnO_3$, as already explained in the methodology section, section 2. The usual expectation is [14] that $x_{ll'} = l + l' + 1$, therefore suggesting 3, 3 and 4 as the values of x_{sd}, x_{pp} and x_{pd} respectively. It has been empirically suggested by Harrison [14] that the optimal choices for these three parameters are 3.5, 2 and 3.5 respectively. Our analysis yields the best choices for x_{sd}, x_{pp} and x_{pd} as 2.5, 3.06 and 3.5 respectively.

It is well known that the gross electronic structures of such oxides can be described in terms of the electronic interaction strengths, such as the various hopping interactions, the charge-transfer energy (Δ), intra-atomic Coulomb interaction strength within the transition metal d manifold (U_{dd}), and the exchange interaction strength (J). It is to be noticed that the bare energies, ϵ_p and ϵ_d, obtained by the above analysis of the LMTO calculations are not the ionization energies of the respective orbitals, and thus the difference ($\epsilon_d - \epsilon_p$) cannot be directly related to the bare charge-transfer energy, Δ. However, these quantities are interrelated. In order to see this connection, we first note that the energy of the ith orbital in any LDA calculation is given by the partial derivative of the total energy (E) with respect to the occupancy (n_i) of that level [17], i.e., $\epsilon_i = \partial E/\partial n_i$

Moreover, the total energy can be expanded in a Taylor series involving the occupancies of the various levels as

$$E(\cdots n_i \cdots) = a_0 + \sum_i a_1^i n_i + \sum_{i \geqslant j} a_2^{ij} n_i n_j + \cdots. \tag{1}$$

If we retain terms up to the second order, it can easily be shown [7] that the coefficients a_2^{ij} are related to various Coulomb interaction strengths. In the present context, it can also be shown that the up-spin and down-spin charge-transfer energies are given by

$$\Delta_\uparrow = E(n_{d\uparrow} + 1, n_{p\uparrow} - 1) - E(n_{d\uparrow}, n_{p\uparrow}) = \epsilon_{d\uparrow} - \epsilon_{p\uparrow} + \frac{1}{2}U_{dd} \tag{2}$$

and

$$\begin{aligned}\Delta_\downarrow &= E(n_{d\downarrow} + 1, n_{p\downarrow} - 1) - E(n_{d\downarrow}, n_{p\downarrow}) \\ &= \epsilon_{d\downarrow} - \epsilon_{p\downarrow} + \frac{1}{2}U_{dd} = (\epsilon_{d_\uparrow} - \epsilon_{p_\uparrow}) + \epsilon_{pol} + \frac{1}{2}U_{dd}.\end{aligned} \tag{3}$$

Thus, while the present estimates of $\epsilon_{d\uparrow} - \epsilon_{p\uparrow}$ given in table 1 do not uniquely define the charge-transfer energies, they define Δ as a function of U_{dd} in terms of the values of $\epsilon_{d\uparrow} - \epsilon_{p\uparrow}$ and ϵ_{pol} in table 1.

It is to be noticed that we can combine the equations (2) and (3) and obtain

$$\Delta_\uparrow - \Delta_\downarrow = \epsilon_{pol}. \tag{4}$$

However, it is easily seen that

$$\Delta_\uparrow - \Delta_\downarrow = NJ \tag{5}$$

where N is the number of d electrons and J is the intra-atomic exchange interaction strength. Thus, ϵ_{pol}/N provides a direct estimate for J. We obtain approximately 0.88, 0.93 and 0.76 eV as the estimates for J for $LaCrO_3$, $LaMnO_3$ and $LaFeO_3$ respectively; these estimates are consistent with earlier estimates of J obtained from spectroscopic data. It is very interesting to note that the strength of J is the highest for $LaMnO_3$ among these three compounds; the importance of a large J in determining the unusual properties of $LaMnO_3$ has already been discussed [5].

To summarize, we have performed *ab initio* LSDA band-structure calculations for $LaCrO_3$, $LaMnO_3$ and $LaFeO_3$ for the observed magnetic structure using real crystal

structure information. Analysis of the band dispersions with a tight-binding model yields estimates of various interaction parameters that govern the electronic structure of these compounds. The strengths of the various interactions exhibit a systematic trend across the series. We estimate the intra-atomic exchange interaction strength, J, to be 0.88, 0.93 and 0.76 eV for M = Cr, Mn and Fe in $LaMO_3$.

Acknowledgments

DDS thanks Drs M Methfessel, A T Paxton, and M van Schiljgaarde for making the LMTO-ASA band-structure program available and Dr S Krishnamurthy for initial help in setting up the LMTO-ASA program. NS and PM thank the CSIR, Government of India, for financial support.

References

[1] Sawatzky G A and Allen J W 1984 *Phys. Rev. Lett.* **53** 2239
Zannen J, Sawatzky G A and Allen J W 1985 *Phys. Rev. Lett.* **55** 418
[2] Sarma D D, Krishnamurthy H R, Nimkar S, Ramasesha S, Mitra P P and Ramakrishnan T V 1992 *Pramana* **38** L531
Nimkar S, Sarma D D, Krishnamurthy H R and Ramasesha S 1993 *Phys. Rev.* B **48** 7355
[3] van der Laan G, Westra C, Haas C and Sawatzky G A 1981 *Phys. Rev.* B **23** 4369
Zaanen J, Westra C and Sawatzky G A 1986 *Phys. Rev.* B **33** 8060
Sarma D D 1988 *Phys. Rev.* B **37** 7948
Chainani A, Mathew M and Sarma D D 1993 *Phys. Rev.* B **48** 14 818
Bocquet A E, Mizokawa T, Morikawa K, Fujimori A, Barman S R, Maiti K, Sarma D D, Tokura Y and Onoda M 1996 *Phys. Rev.* B **53** 1161
[4] Sarma D D 1996 *J. Phys. Soc. Japan* **65** 1325
[5] Sarma D D, Shanthi N and Mahadevan P 1996 *Phys. Rev.* B **54** 1622
Sarma D D *et al* 1996 *Phys. Rev.* B **53** 6873
[6] Sarma D D, Shanthi N, Barman S R, Hamada N, Sawada H and Terakura K 1995 *Phys. Rev. Lett.* **75** 1126
[7] Mahadevan P, Shanthi N and Sarma D D 1996 *Phys. Rev.* B **54** 11 199
Sarma D D 1991 *Rev. Solid State Sci.* **5** 461
[8] Anderson O K and Kasowski R V 1971 *Phys. Rev.* B **4** 1064
Anderson O K 1973 *Solid State Commun.* **13** 133
Anderson O K 1975 *Phys. Rev.* B **12** 3060
[9] Khattak C P and Cox D E 1977 *J. Appl. Crystallogr.* **10** 405
[10] Elemans J B A A, van Larr B, van der Veen K R, and Loopstra B O 1971 *J. Solid State Chem.* **3** 238
[11] Marezio M and Dernier P D 1971 *Mater. Res. Bull.* **6** 23
[12] Slater J C and Koster G F 1954 *Phys. Rev.* **94** 1498
[13] Mattheiss L F 1970 *Phys. Rev.* B **2** 3918
[14] Harrison W A 1989 *Electronic Structure and Properties of Solids* (New York: Dover)
[15] Andersen O K, Klose W and Nohl H 1978 *Phys. Rev.* B **17** 1209
[16] Ballhausen C J 1962 *An Introduction to Ligand Field Theory* (New York: McGraw-Hill)
[17] Slater J C and Wood J H 1971 *Int. J. Quantum Chem.* **45** 3
Slater J C, Wilson T M and Wood J H 1969 *Phys. Rev.* **179** 28